

Green Synthesis of Silver Nanoparticles Using *Coriandrum sativum* Extract and Their Antioxidant, Anti-inflammatory and Antibacterial Activities Against UTI Pathogens

G Dinesh, Lakshmi Thangavelu*, S Rajeshkumar, Pradeep Manigandan
Centre for Global Health Research, Saveetha Medical College and Hospitals, Saveetha
Institute Medical and Technical Sciences, Saveetha University, Chennai, 602105,
Tamil Nadu, India

Abstract

This study explored the green synthesis of silver nanoparticles (AgNPs) utilizing *Coriandrum sativum* extract and investigated their potential applications in terms of antibacterial and antioxidant activities. UV-visible absorption spectra revealed a distinctive absorption peak at 450 nm, indicating successful AgNPs synthesis and stabilization with *Coriandrum sativum* extract and the TEM analysis revealed the shape to be spherical and size was found to range between 5-25 nm. Antibacterial assays revealed concentration-dependent zones of inhibition against *Staphylococcus aureus*, *Escherichia coli*, *Pseudomonas sp.*, and *Klebsiella sp.*, confirming the efficacy of *Coriandrum sativum*-mediated AgNPs as antibacterial agents. The AgNPs exhibited significant antioxidant properties, with concentration-dependent scavenging activities observed in the DPPH, hydrogen peroxide, and FRAP assays. Protein denaturation assays revealed concentration-dependent effects, suggesting potential applications in biological and medicinal contexts. Additionally, membrane stabilization assays revealed the robust concentration-dependent impact of *Coriandrum sativum*-mediated AgNPs, underscoring their promising role in diverse applications, from antibacterial treatments to antioxidant therapies and protein stability studies.

Keywords: Antioxidant Agent, Anti-inflammatory Agent, Green Synthesis, Silver Nanoparticles, Urinary Tract Pathogens.

Introduction

Urinary tract infections (UTIs) are prevalent bacterial infections that impact the urinary system, including the bladder, urethra, and kidneys. These infections, varying from uncomplicated to complicated, are commonly caused by bacteria such as UPEC and other pathogens. Factors contributing to increased UTI risk include low estrogen levels, diabetes, and urinary catheterization [1,2]. Recent data from the NHS and the UK Health Security Agency highlight that UTIs have resulted in over 800,000 hospital admissions in the UK over the last five years, particularly affecting older adults. UTI symptoms include frequent

urination, a painful or burning sensation during urination, cloudy urine, and back pain. To prevent UTIs, individuals are advised to stay hydrated, avoid holding their urine for extended periods, and maintain good hygiene practices [3].

Antibiotic resistance in urinary tract infections (UTIs) is a global concern that continues to escalate. This increasing resistance is attributed to the inappropriate use and overuse of antibiotics, not only in human medicine but also in livestock. The misuse of these medications contributes significantly to the development of resistance in bacteria [4]. Silver nanoparticles (AgNPs) have exhibited

promising potential in the treatment of urinary tract infections (UTIs) owing to their antibacterial properties. The mechanism of action involves the release of silver ions, which can attach to the bacterial cell wall and cytoplasmic membrane, thereby increasing permeability and disrupting the bacterial envelope [5]. Silver ions further deactivate respiratory enzymes, leading to the generation of reactive oxygen species and interference with adenosine triphosphate production [6]. Moreover, silver ions can interact with sulfur and phosphorus in DNA, hindering the process of replication and cell reproduction [7]. In addition to their application in UTI treatment, AgNPs have been extensively studied for their potential in diverse areas, such as drug delivery, medical imaging, molecular diagnostics, and various therapeutic applications. These include the development of surgical mesh, artificial joint replacements, wound dressings, and medicaments for wound healing [8].

The green synthesis of silver nanoparticles (AgNPs) from *Coriandrum sativum* (CS) leaf extract is a swift and environmentally friendly method that yields nanoparticles with consistent sizes and shapes. This process involves the use of plant extracts, which lack chemical compounds on their surface and are deemed nonharmful to human cells [9,10]. Coriander, scientifically known as *Coriandrum sativum*, is an annual herb belonging to the family *Apiaceae*. Native to the Mediterranean Basin, it is widely recognized and utilized as both a spice and an herb in various global cuisines [9]. The edible parts of plants include fresh leaves and dried seeds, which are commonly incorporated into cooking. In addition to its culinary applications, coriander has garnered attention for its potential health benefits and therapeutic properties. Like coriander, which is rich in vitamin C, calcium, magnesium, potassium, and iron, coriander also possesses essential oils with potential antibacterial effects [11,12]. Traditional medicine has historically employed coriander

for managing conditions such as anxiety, constipation, diabetes, indigestion, parasite infections, irritable bowel syndrome (IBS), and skin irritation[13]. Some of the major phytochemicals present in the plant *Coriandrum sativum* was observed to be 1,6-Octadien-3-ol,3,7-dimethyl, 1,6-Octadien-3-ol,3,7-dimethyl, 2-aminobenzoate, Bicyclo [2.2.1]heptan-2-one,1,7,7-trimethyl, Geranyl vinyl ether, 9,10-Secocholesta-5,7,10(19)-triene-3,24,25-triol, Ascorbic acid 2,6-dihexadecanoate, 7aH-Cyclopenta[a]cyclopropa[f]cycloundecene, which are responsible for the biological activities including Anti-inflammatory, antiseptic, antidepressant, Immune enhancement, antimicrobial activity, Anti-cancer, hepatoprotective, Antimetastatic, anti-invasive, and antioxidant action. Furthermore, the phytochemicals present in the respective plant may enhance the activities of CS-AgNPs [14].

The current study delves into the innovative synthesis of silver nanoparticles (AgNPs) employing *Coriandrum sativum* extract as a dual-functioning green reducing and stabilizing agent. In addition to the synthesis aspect, investigations have explored the multifaceted properties of these nanoparticles. The evaluation of their antibacterial, antioxidant, and anti-inflammatory activities adds significant value to the study, highlighting the potential of AgNPs derived from *Coriander sativum* as promising candidates for various applications in medicine and related fields.

Materials and methods

Collection and Preparation of *Coriander sativum* Leaf Extract

Coriander sativum leaves were procured from a local supermarket near Poonamallee. Next, the *Coriander sativum* leaves were thoroughly washed with tap water, followed by an additional rinse with distilled water. The cleaned *Coriander sativum* leaves were subsequently allowed to air dry for one hour at room temperature. Once dried, 10 grams of the

leaves were precisely weighed and crushed using a mortar and pestle. The resulting extract was filtered through Whatman No:1 filter paper to obtain a refined solution. This filtered extract was then carefully stored in a refrigerator for subsequent stages of nanoparticle synthesis.

Green Synthesis of Silver Nanoparticles

A solution comprising 1 mM silver nitrate was dissolved in 60 mL of distilled water, and subsequently, 40 mL of filtered *Coriander sativum* leaf extract was added to this mixture. The resulting reaction mixture was placed on a magnetic stirrer operating at 700 rpm and maintained for a duration ranging from 24--56 hours. Simultaneously, UV-visible spectrophotometer readings were consistently recorded throughout this period to verify and confirm the synthesis process.

Characterization of AgNPs

The characterization of the green-synthesized silver nanoparticles was conducted via a UV-visible spectrophotometer. This analytical tool allows for a thorough examination of the optical properties of the nanoparticles. Green synthesized AgNPs were analyzed using a UV visible spectrometer from the wavelength 280-680 nm. The interior structure of the synthesized AgNPs TEM analysis.

Antibacterial Activity

The antibacterial activity of the green synthesized AgNPs was evaluated via the agar well diffusion technique. Mueller Hinton agar plates were prepared and sterilized by autoclaving at 121°C for 15–20 minutes. After sterilization, the medium was poured onto the surface of sterile Petri plates and allowed to cool to room temperature. The bacterial suspensions (*Staphylococcus aureus*, *Klebsiella* sp., *Escherichia coli*, and *Pseudomonas aeruginosa*) were spread evenly onto agar plates with sterile cotton swabs. Wells 9 mm in diameter were created on agar plates via a sterile polystyrene tip. The wells were then

filled with different concentrations (25 µg, 50 µg, 100 µg) of AgNPs. The plant extract without silver nitrate was used as a control group. The plates were incubated at 37°C for 24 hours and evaluated by measuring the diameter of the inhibition zone surrounding the wells. The diameter of the zone of inhibition was measured via a ruler and recorded in millimetres (mm) [15].

Antioxidant Activity

DPPH Assay

The in vitro DPPH (1,1-diphenyl-2-picrylhydrazyl) assay is commonly employed to assess the antioxidant properties of various compounds, including plant extracts. This method relies on the compound's capacity to neutralize this free radical, stable, dark-colored crystalline compound. The reduction of DPPH radicals into DPPH-H, a colorless or light yellow compound, serves as an indicator of the antioxidant's ability to neutralize free radicals, and its free radical scavenging activity (RSA) can be evaluated.

To create the stock solution, 24 milligrams of DPPH were dissolved in 100 mL of methanol, resulting in a filtrated mixture with an absorbance of approximately 0.973 at 517 nm. Different concentrations of coriander leaf extract containing silver nanoparticles (10 µg/mL- 50 µg/mL) were then combined with 3 mL of this DPPH solution, and the mixture was incubated in complete darkness for 30 minutes. The absorbance was subsequently measured at 517 nm, and the percentage of antioxidant activity was subsequently calculated via the following formula:

$$\text{Percentage of antioxidant activity} \\ = [(Ac - As) \div Ac] \times 100$$

where Ac represents the control reaction absorbance and As represents the test sample absorbance.

H₂O₂ Assay

In the in vitro hydrogen peroxide radical scavenging assay, coriander leaf-mediated

silver nanoparticles (AgNPs) were used as the test substance, and the following steps were followed. Hydrogen peroxide (H₂O₂) was prepared as a stock solution at a concentration of 3% (w/v). Horseradish peroxidase (HRP) was used as the peroxidase enzyme, with a stock solution prepared at a concentration of 1 mg/mL in phosphate buffer (pH 7.4). A substrate solution containing 4-aminoantipyrine (4-APA), which changes color upon reduction, and phosphate buffer (pH 7.4) as the buffer solution was also prepared. Control solutions without the test substance were included for comparison.

For the test solution, coriander leaf extract-mediated AgNPs were dissolved in an appropriate solvent (distilled water) to achieve the desired concentration (10 µg/mL-- 50 µg/mL). The assay mixture, comprising hydrogen peroxide, HRP, the substrate solution, and the test solution, was prepared in a 96-well plate. A uniform final volume in each well was ensured. The assay mixture was then incubated at 37°C for 30 minutes to facilitate the reduction of hydrogen peroxide by the enzyme and the scavenging of hydrogen peroxide by the coriander-mediated AgNPs.

After incubation, the absorbance of each well was measured at 504 nm via a spectrophotometer, which corresponds to the color change of the substrate solution. Data analysis involved comparing the absorbance values of the test solution wells with those of the control wells. The percentage of inhibition of color change was calculated via the following formula:

$$\text{Percentage of Inhibition} = \frac{(\text{Absorbance of Control} - \text{Absorbance of Test Solution})}{\text{Absorbance of Control}} \times 100$$

The percentage of inhibition obtained serves as an indicator of the scavenging efficiency of coriander-mediated AgNPs. A higher percentage suggests superior antioxidant activity, indicating the ability of the test substance to effectively neutralize or reduce the activity of hydrogen peroxide [16,17].

FRAP Assay

The ferric-reducing antioxidant power (FRAP) assay is a widely utilized technique for assessing the total antioxidant capacity of biological samples. In this method, a FRAP reagent is prepared by combining 300 mM acetate buffer (pH 3.6), 10 mM TPTZ (2,4,6-tris(2-pyridyl)-s-triazine) in 40 mM HCl, and 20 mM FeCl₃.6H₂O in a 10:1:1 ratio.

To conduct the FRAP assay, varying concentrations (10 µg/mL--50 µg/mL) of green synthesized silver nanoparticles and standards were dispensed into a 96-well plate in triplicate, with approximately 20 µL each. Two hundred microliters of the prepared FRAP reagent were subsequently added to each well, and the plate was incubated at 37°C for 30 minutes. The absorbance at 593 nm was then measured for each well via a microplate reader.

The FRAP value for each sample or standard was determined by comparing the absorbance to a standard curve generated using known concentrations of a standard antioxidant, such as Trolox. The FRAP assay assesses the capacity of antioxidants in the samples to convert Fe³⁺ to Fe²⁺ within the FRAP reagent, resulting in a color change that is directly proportional to the antioxidant capacity of the sample. This method offers a quantitative measure of the antioxidant activity present in biological samples, making it a valuable tool for evaluating the overall antioxidant potential of green-synthesized silver nanoparticles and other substances.

Anti-inflammatory Activity

Green-synthesized silver nanoparticles were tested for their anti-inflammatory activity via three assays: the bovine serum albumin denaturation assay, egg albumin denaturation assay, and membrane stabilization assay.

Bovine Serum Albumin Denaturation Assay

A solution containing 0.45 mL of bovine serum albumin was prepared by mixing it with 0.05 mL of *Coriander sativum*-mediated AgNPs, which were present at various concentrations ranging from 10 to 50 µg/mL. The pH of the solution was subsequently adjusted to 6.3. The mixture was then incubated at room temperature for 10 minutes. Next, the samples were subjected to a 30-minute incubation period in a water bath at 55°C. For comparison purposes, diclofenac sodium was utilized as the standard group, whereas dimethyl sulfoxide served as the control. Finally, the samples were analyzed spectrophotometrically at a wavelength of 660 nm.

The percentage of protein denaturation was determined via the following equation:

$$\frac{\text{Percentage of inhibition} = \frac{\text{Absorbance of Control} - \text{Absorbance of sample}}{\text{Absorbance of control}} \times 100$$

Egg Albumin Denaturation Assay

For the egg albumin denaturation assay, a reaction mixture was prepared by mixing 0.2 mL of fresh egg albumin with 2.8 mL of phosphate buffer. To this mixture, *Coriander sativum*-mediated AgNPs nanoparticles were added at various concentrations ranging from 10 to 50 µg/mL. The pH of the solution was then adjusted to 6.3. The mixture was subsequently incubated at room temperature for 10 minutes. Next, the samples were subjected to a 30-minute incubation period in a water bath at 55°C. For comparison, diclofenac sodium was employed as the standard group, whereas dimethyl sulfoxide was utilized as the control. Finally, the samples were analysed spectrophotometrically at a wavelength of 660 nm.

The percentage of protein denaturation was determined via the following equation:

$$\frac{\text{Percentage of inhibition} = \frac{\text{Absorbance of Control} - \text{Absorbance of sample}}{\text{Absorbance of control}} \times 100$$

Membrane Stabilization Assay

An in vitro membrane stabilization assay was used to evaluate the membrane-stabilizing properties of the compounds. This assay assessed the potential of the synthesized AgNPs from *Coriander sativum* leaves (10–50 µg/mL) to prevent the disruption of cell membranes and the subsequent release of intracellular contents. The assay utilized Tris-HCl buffer, human red blood cells (RBCs), phosphate-buffered saline (PBS), centrifuge tubes, and a UV–visible spectrophotometer.

Preparation of RBC Suspensions

Fresh human blood was collected in a sterile tube with anticoagulants. After the blood was centrifuged at 1,000 × g for 10 minutes at room temperature, the RBCs were separated. The RBCs were washed three times with PBS and resuspended in Tris-HCl buffer to create a 10% (v/v) RBC suspension.

Assay Procedure

One milliliter of the RBC suspension was placed into each centrifuge tube, followed by the addition of different concentrations of AgNPs. The tubes were gently mixed and incubated at 37°C for 30 minutes. After the tubes were centrifuged at 1,000 rpm for 10 minutes at room temperature, the absorbance of the supernatant was measured at 540 nm via a UV–visible spectrophotometer. The percentage inhibition of hemolysis was calculated as follows:

$$\frac{\text{Percentage of inhibition} = \frac{\text{Absorbance of Control} - \text{Absorbance of sample}}{\text{Absorbance of control}} \times 100$$

Here, the OD control is the absorbance of the RBC suspension without the test compound(s), and the OD sample is the absorbance of the RBC suspension with the test compound.

Results and Discussion

Visual Observation

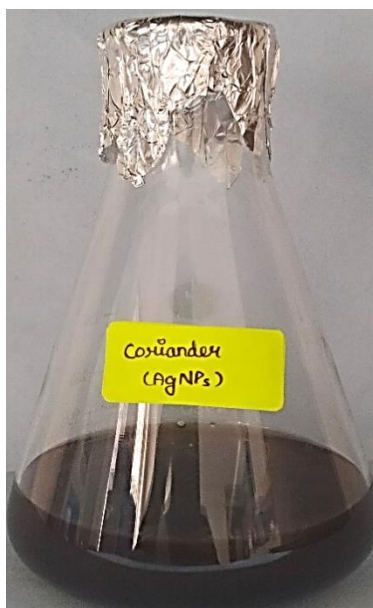


Figure 1. Visual Observation of *Coriandrum sativum*-Mediated AgNPs Production

Visual examination of the reaction mixture during the green synthesis of silver nanoparticles (AgNPs) using *Coriandrum sativum* extract revealed distinct color changes over time, as depicted in Figure 1. Initially, at the 1-hour mark, the solution exhibited a pale brown hue, suggesting the onset of nanoparticle synthesis. Subsequent visual assessments at 24 hours and 48 hours indicated a gradual deepening of the color, reflecting the progressive formation and growth of AgNPs within the reaction period. The most

pronounced color change occurred between 48 and 56 h when the solution transitioned to a dark reddish-brown color. This final color transformation is indicative of the successful synthesis and stabilization of silver nanoparticles, with the observed dark reddish-brown hue characteristic of the surface plasmon resonance (SPR) band associated with silver nanoparticles.

UV-Visible Spectroscopy

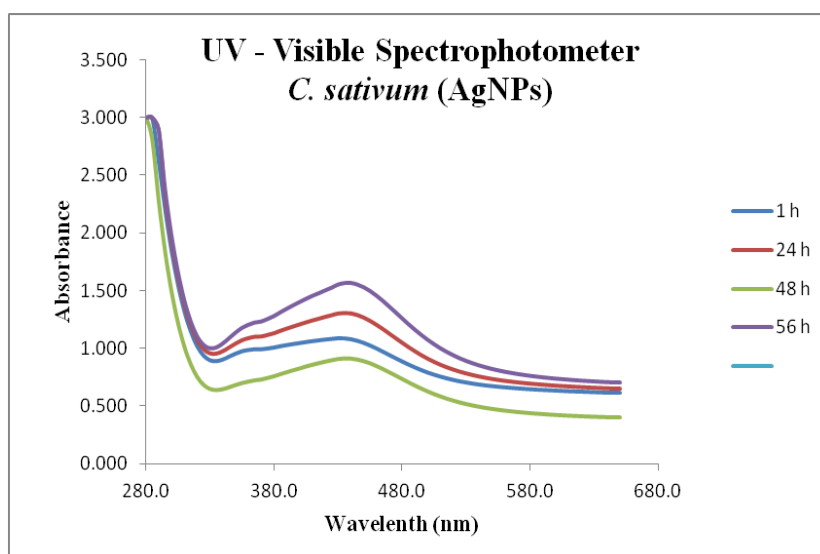


Figure 2. UV-Visible Spectra of the Green-Synthesized Silver Nanoparticles

The UV–visible absorption spectra of the *Coriander sativum*-mediated silver nanoparticles (AgNPs) were acquired over a wavelength range of 280–680 nm at different time intervals, namely, 1 h, 24 h, 48 h, and 56 h, as shown in Figure 1. The spectral analysis revealed distinct absorption peaks, with the maximum absorption observed at 450 nm. At the initial measurement time of 1 h, a preliminary absorption peak was observed, indicating the onset of nanoparticle synthesis. Subsequent measurements at 24 h and 48 h revealed a gradual increase in intensity, suggesting the progressive formation and growth of silver nanoparticles within the reaction period. The most prominent result was obtained at 56 h, where the UV–visible spectrum exhibited a well-defined absorption

peak at 450 nm, indicating the presence of silver nanoparticles. This peak corresponds to the surface plasmon resonance (SPR) band characteristic of silver nanoparticles, indicating their successful synthesis and stabilization with the *Coriander sativum* extract. The choice of *Coriander sativum* as a green reducing and stabilizing agent is validated by the distinctive absorption peak at 450 nm, demonstrating its efficacy in mediating the synthesis of silver nanoparticles. The narrow and well-defined nature of the absorption peak further indicates the uniform size distribution of the nanoparticles, emphasizing the reproducibility and consistency of the green synthesis process.

TEM Analysis

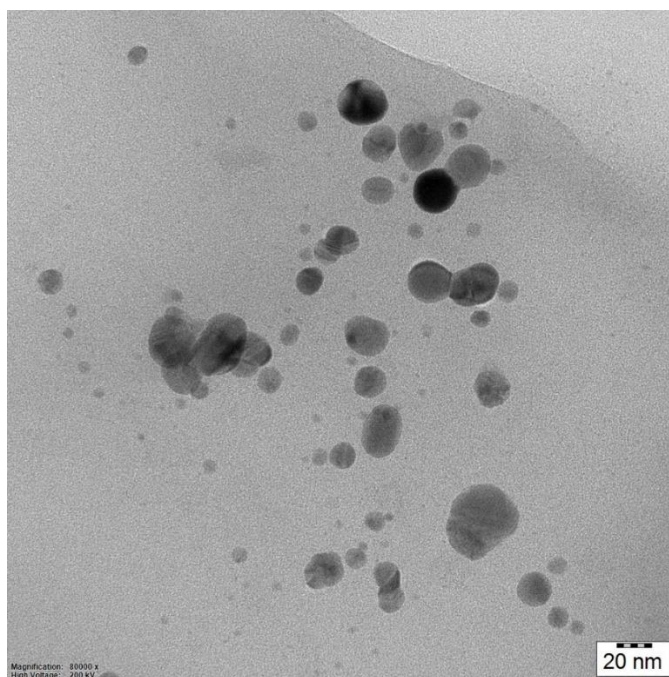


Figure 3. Transmission Electron Microscopy Analysis of Green Synthesized AgNPs

TEM, or transmission electron microscopy, is an additional important technique for characterizing nanomaterials. The size, shape, and distribution of the particles may be determined quantitatively. Similar to SEM, TEM is an electronic spectroscopic imaging

method, but with a better resolution. As shown in Figure 3, the study findings reveal that the size of the green synthesized AgNPs was found to be 16 nm ranging between 5-25 nm. The shape of the AgNPs was noted as spherical, and oval

Antibacterial Activity Against UTI Pathogens

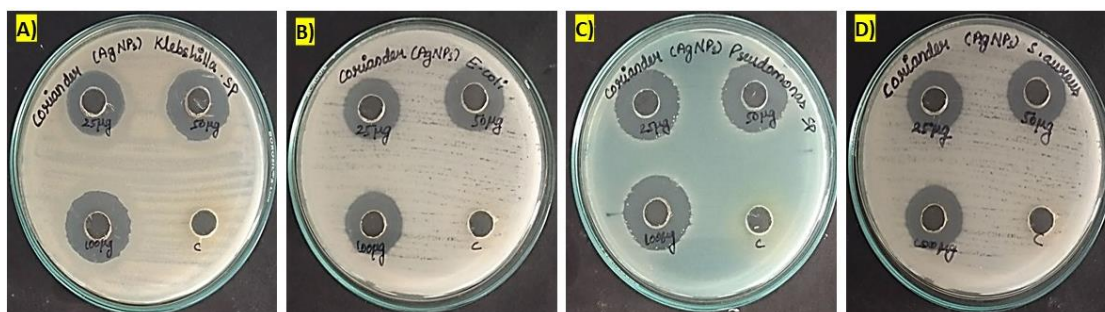


Figure 4. Antibacterial Activity Against Urinary Tract Pathogens Via the Agar Well Diffusion Technique: a) *Klebsiella* sp., b) *E. coli*, C) *Pseudomonas* sp., D) *S. aureus*

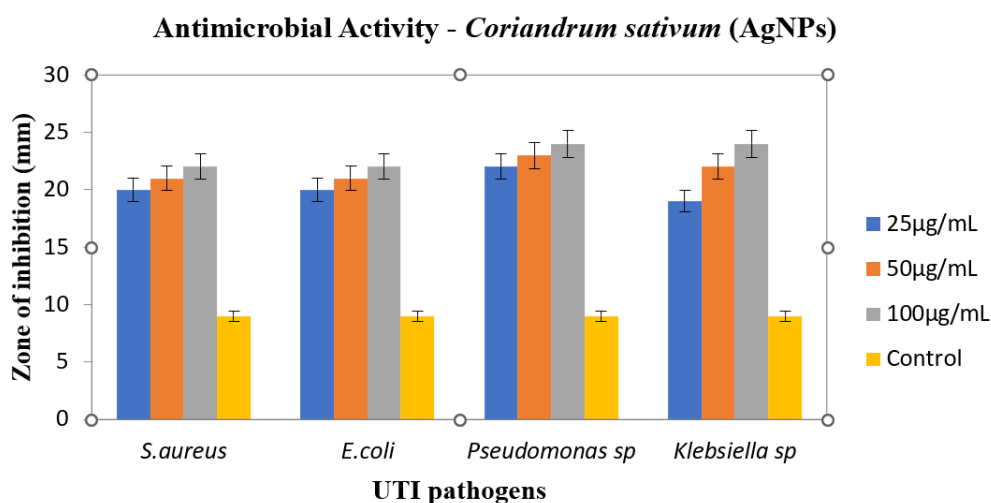


Figure 5. Antibacterial Activity of Green-Synthesized AgNPs Against Urinary Tract Pathogens

The agar well diffusion technique was employed to thoroughly investigate the antibacterial activity of *Coriander sativum*-mediated AgNPs against four urinary tract infection (UTI) pathogens: *Staphylococcus aureus*, *Escherichia coli*, *Pseudomonas* sp., and *Klebsiella* sp. Three different concentrations of CS-AgNPs (25 µg/mL, 50 µg/mL, and 100 µg/mL) were assessed, and the results revealed distinct zones of inhibition, indicating the extent of bacterial growth inhibition around each well (Figure 4).

As shown in Figure 5, for *S. aureus*, the zones of inhibition were 20.5 ± 0.3 mm, 21.2 ± 0.4 mm, and 22.0 ± 0.5 mm at concentrations of 25 µg/mL, 50 µg/mL, and 100 µg/mL, respectively. The control group presented a zone of inhibition of 9.2 ± 0.2 mm. Similarly, for *E. coli*, the zones of inhibition were 20.3 ± 0.2 mm, 21.0 ± 0.3 mm, and 21.8 ± 0.4 mm, whereas the control group presented a zone of inhibition of 9.1 ± 0.2 mm. For *Pseudomonas* sp., the zones of inhibition were 22.2 ± 0.6 mm, 23.1 ± 0.7 mm, and 24.5 ± 0.8 mm, with the control group presenting a zone of inhibition of 9.3 ± 0.3 mm. Finally, for *Klebsiella* sp., the zones of inhibition were 19.8 ± 0.4 mm, 22.3 ± 0.5 mm, and 24.2 ± 0.6 mm, with the control group exhibiting a zone of inhibition of 9.0 ± 0.1 mm. These detailed findings revealed a clear concentration-dependent antibacterial effect of these green-mediated AgNPs against all tested UTI pathogens, confirming their potential as effective antibacterial agents for combating urinary tract infections.

Antioxidant Activity

DPPH Assay

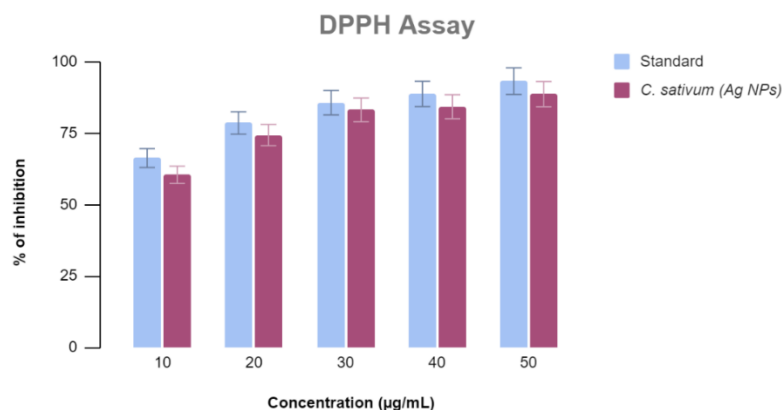


Figure 6. DPPH Assay of *Coriander sativum*-Mediated AgNP Production

As shown in Figure 6, the antioxidant activity of the *Coriandrum sativum* silver nanoparticles (Ag NPs) was assessed via the DPPH assay. This assay was conducted at various concentrations, specifically 10 µg/mL, 20 µg/mL, 30 µg/mL, 40 µg/mL, and 50 µg/mL. The standard antioxidant, which was represented by a concentration of 10 µg/mL, initially demonstrated a DPPH scavenging activity of 66.25%. As the concentration of the antioxidant increased, a proportional increase in its antioxidant activity was observed. This trend peaked at the highest concentration tested, where the antioxidant activity reached 93.15%. In comparison, the *C. sativum* Ag NPs exhibited significant DPPH scavenging activity across all the concentrations tested. At a concentration of 10 µg/mL, the *C. sativum* Ag NPs displayed a DPPH scavenging activity of 60.4%. This activity increased progressively, reaching 88.6% at the highest concentration of 50

µg/mL. These results indicate that both the standard antioxidant and the *C. sativum* Ag NPs possess notable antioxidant properties. Compared with the standard antioxidant ascorbic acid, the *C. sativum* Ag NPs demonstrated comparable or even superior DPPH scavenging activity at certain concentrations. These findings suggest that *C. sativum* Ag NPs could serve as effective natural antioxidants, offering a promising alternative for antioxidant applications. The trend of increasing antioxidant activity with increasing concentration for both the standard antioxidant and the *C. sativum* Ag NPs suggests that the antioxidant activity of these substances may be concentration dependent. This finding is significant because it highlights the potential for optimizing the concentration of *C. sativum* Ag NPs for specific applications, where the desired antioxidant activity can be achieved.

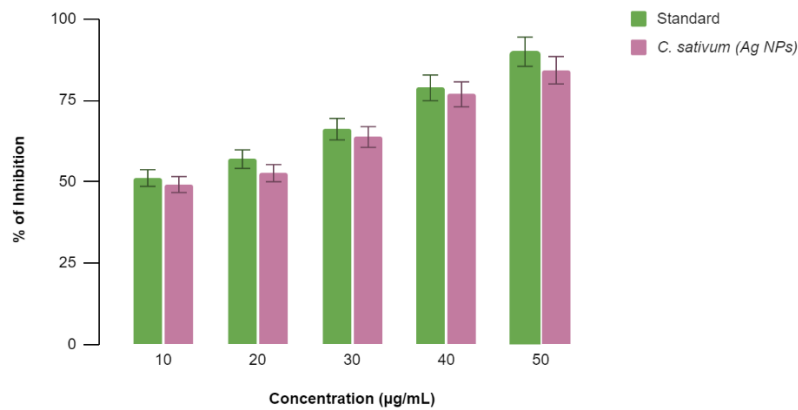


Figure 7. H₂O₂ Assay of *Coriander sativum*-Mediated AgNP Production

As shown in Figure 7, the hydrogen peroxide (H₂O₂) scavenging potential of *C. sativum* Ag NPs was assessed via the H₂O₂ assay at concentrations of 10 µg/mL, 20 µg/mL, 30 µg/mL, 40 µg/mL, and 50 µg/mL. A standard antioxidant (ascorbic acid) was also included for comparison. At the lowest concentration of 10 µg/mL, the standard antioxidant exhibited an H₂O₂ scavenging activity of 51.1%. The H₂O₂ scavenging activity increased progressively with increasing concentration, reaching 89.9% at 50 µg/mL. *C. sativum* Ag NPs demonstrated notable H₂O₂ scavenging activity across all the

concentrations tested. Starting at 49.1% H₂O₂ at 10 µg/mL, the H₂O₂ scavenging activity increased to 84.2% at the highest 50 µg/mL concentration. A comparison of the standard and *C. sativum* Ag NPs revealed a consistent and dose-dependent increase in H₂O₂ scavenging activity. These results highlight the potential antioxidative capabilities of *C. sativum* Ag NPs, indicating their effectiveness in neutralizing hydrogen peroxide radicals.

FRAP Assay

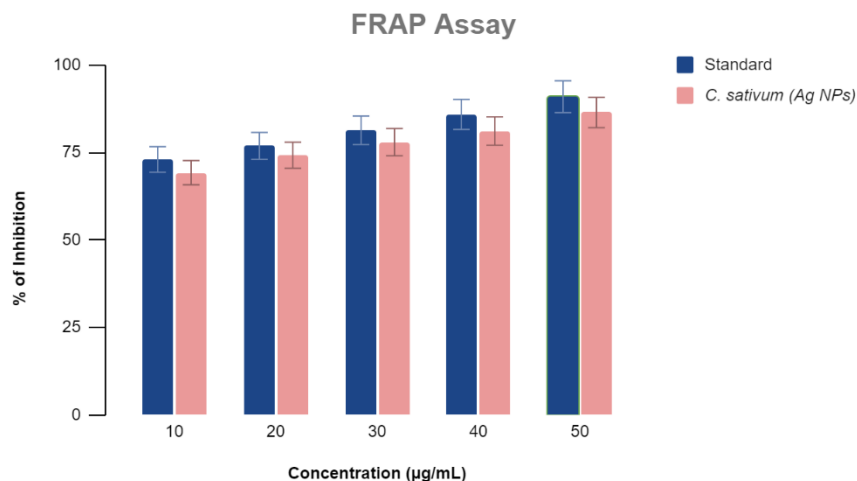


Figure 8. FRAP Assay of the Green-Synthesized AgNPs

As shown in Figure 8, a ferric reducing antioxidant power (FRAP) assay was conducted to evaluate the antioxidant activity of the standard (Trolox) and *Coriandrum sativum*-mediated silver nanoparticles (Ag NPs). The concentration–response relationships were

assessed across various concentrations (10 µg/mL, 20 µg/mL, 30 µg/mL, 40 µg/mL, and 50 µg/mL). The results revealed a concentration-dependent increase in the FRAP values for both the standard and *C. sativum* (Ag NP) samples. At a concentration of 10 µg/mL,

the standard presented a FRAP value of 72.98 $\mu\text{g/mL}$, whereas *C. sativum* (Ag NPs) presented a slightly lower value of 69.2 $\mu\text{g/mL}$. As the concentration increased, both the standard and *C. sativum* (Ag NP) samples exhibited a progressive increase in FRAP. At 20 $\mu\text{g/mL}$, the standard solution displayed a FRAP value of 76.84 $\mu\text{g/mL}$, surpassing the corresponding value for *C. sativum* (Ag NPs) at 74.18 $\mu\text{g/mL}$. This trend continued, with the FRAP values for both the standard and *C. sativum* (Ag NPs) increasing at each subsequent concentration. At the highest concentration tested (50 $\mu\text{g/mL}$), the standard solution presented a FRAP value of

90.89 $\mu\text{g/mL}$, while *C. sativum* (Ag NPs) presented a value of 86.38 $\mu\text{g/mL}$. The observed results suggest that both the standard and *C. sativum* (Ag NPs) possess significant ferric-reducing antioxidant potential, with the standard generally exhibiting a slightly higher FRAP value across all concentrations. These findings support the potential antioxidant activity of *C. sativum* aqueous extract treated with silver nanoparticles, highlighting its ability to reduce ferric ions and suggesting its potential utility as a natural antioxidant agent.

Anti-inflammatory Activity

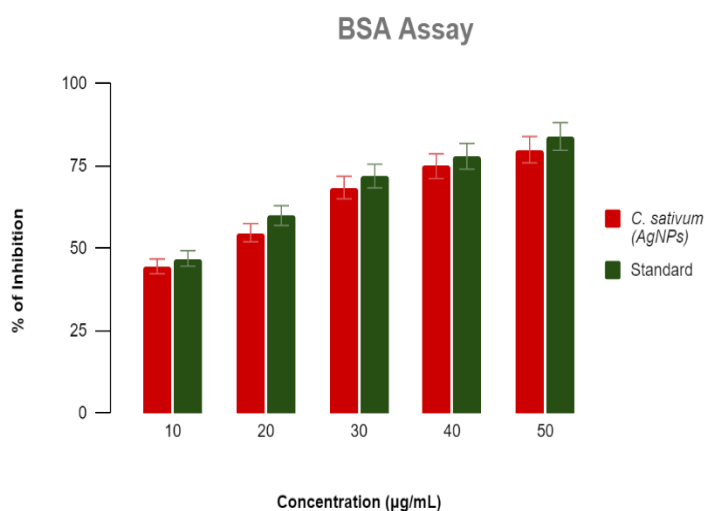


Figure 9. Bovine Serum Albumin Denaturation Assay of Green-Synthesized AgNPs

The bovine serum albumin (BSA) denaturation assay conducted in this study aimed to investigate the impact of various concentrations of *C. sativum*-mediated silver nanoparticles (AgNPs) on the denaturation of BSA, as depicted in Figure 9. The concentrations of *C. sativum* AgNPs tested ranged from 10 $\mu\text{g/mL}$ to 50 $\mu\text{g/mL}$. The results of the denaturation assay were compared with a standard diclofenac sodium denaturation profile to evaluate the effectiveness of *C. sativum* AgNPs in inducing BSA denaturation. The analysis revealed a clear trend: as the concentration of *C. sativum* AgNPs increased, the percentage of BSA denaturation increased. Notably, the denaturation percentages observed

in the presence of *C. sativum* AgNPs are either in the same range or higher than those observed with the standard. This suggests that *C. sativum* AgNPs may have a significant effect on the denaturation of BSA, potentially due to their unique properties and interactions with BSA molecules. These results indicate that *C. sativum* AgNPs could be promising agents for inducing BSA denaturation, with potential applications in various biological and medicinal contexts. The observed increase in denaturation percentages with increasing concentrations of *C. sativum* AgNPs suggests that these nanoparticles may be effective in enhancing the denaturation process, which could be leveraged

for therapeutic purposes or in the study of protein denaturation mechanisms.

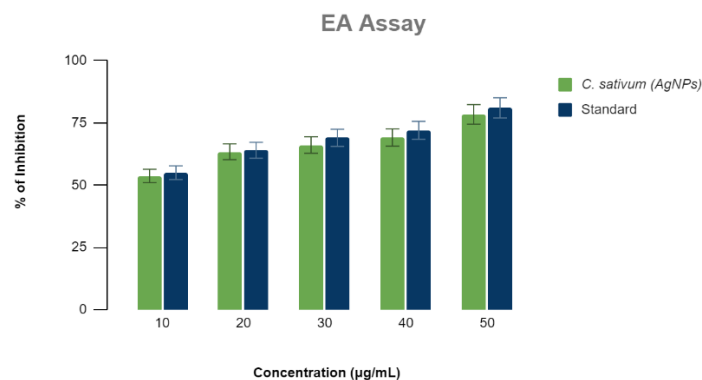


Figure 10. Egg Albumin Denaturation Assay of Green-Synthesized AgNPs

In the egg albumin denaturation assay, the influence of varying concentrations of *Coriandrum sativum* silver nanoparticles (AgNPs) on protein stability was investigated, as shown in Figure 10. The concentrations tested (10 µg/mL, 20 µg/mL, 30 µg/mL, 40 µg/mL, and 50 µg/mL) had concentration-dependent effects on egg albumin denaturation. At 10 µg/mL, the denaturation effect of the *C. sativum* AgNPs (53.7%) was slightly lower than that of the standard (55%). At 20 µg/mL, both *C. sativum* AgNPs (63.4%) and the standard demonstrated comparable

denaturation percentages (64%). The concentration of 30 µg/mL showed a similar trend, with *C. sativum* AgNPs inducing denaturation (66.1%) slightly lower than the standard (69%). At 40 µg/mL, the denaturation percentages for *C. sativum* AgNPs (69.12%) and the standard remained close (72%). Notably, at 50 µg/mL, the denaturation effect of the *C. sativum* AgNPs was more pronounced (78.4%) than that of the standard (81%). These results suggest that *C. sativum* AgNPs impact egg albumin denaturation in a concentration-dependent manner.

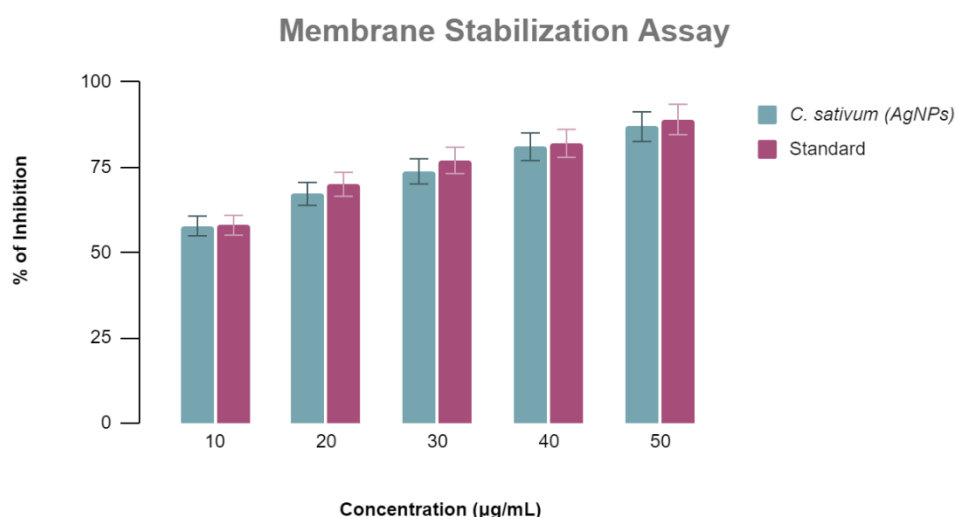


Figure 11. Membrane Stabilization Assay of the Green-Synthesized AgNPs

In the membrane stabilization assay investigating the impact of *Coriandrum sativum*-mediated silver nanoparticles (AgNPs)

on membrane stability, concentrations of 10 µg/mL, 20 µg/mL, 30 µg/mL, 40 µg/mL, and 50 µg/mL were examined, as depicted in Figure

11. These results demonstrate that *C. sativum*-mediated AgNP production has a concentration-dependent membrane stabilization effect. At 10 µg/mL, the percentage of membrane stabilization induced by *C. sativum* AgNPs (57.8%) was comparable to that of the standard (58%). As the concentration increased, the membrane stabilization effects of the *C. sativum* AgNPs became more pronounced, with percentages exceeding those of the standard at higher concentrations. Notably, at 50 µg/mL, the percentage of *C. sativum* AgNP membrane stabilization was 86.9%, surpassing the standard value of 89%.

Discussion

The present study investigated the synthesis of silver nanoparticles (AgNPs) using *Coriander sativum* extract as a green reducing and stabilizing agent and evaluated their potential antibacterial, antioxidant, and anti-inflammatory activities. The distinctive absorption peak at 450 nm in the UV-visible spectra indicated the successful synthesis and stabilization of the AgNPs, which was characterized by a uniform size distribution and the average size of the green synthesized AgNPs was observed as 16 nm ranging from 5-25 nm. Antibacterial assays revealed concentration-dependent zones of inhibition against key urinary tract infection pathogens, suggesting the potential of *Coriandrum sativum*-mediated AgNPs as effective antibacterial agents. The varying inhibitory zones at different concentrations (25 µg/mL, 50 µg/mL, and 100 µg/mL) underscored the concentration-dependent nature of their antibacterial activity. The antioxidant potential of the AgNPs was evident in their concentration-dependent scavenging activities across the DPPH, hydrogen peroxide, and FRAP assays. Notably, the antioxidant efficacy of the AgNPs was comparable or superior to that of standard antioxidants (ascorbic acid), highlighting their potential as effective natural

antioxidants. Protein denaturation assays revealed a concentration-dependent effect of *Coriandrum sativum*-generated AgNPs on protein stability, suggesting their potential applications in modulating protein structure. The observed concentration-dependent denaturation percentages in both the BSA and egg albumin denaturation assays provide insights into their interactions with proteins. Membrane stabilization assays revealed a concentration-dependent membrane stabilization effect, surpassing standard values at higher concentrations. The pronounced membrane stabilization at 50 µg/mL indicates the potential utility of *Coriandrum sativum*-mediated AgNPs in maintaining membrane integrity. Overall, the environmentally friendly *Coriandrum sativum*-mediated AgNPs exhibited concentration-dependent antibacterial, antioxidant, and protein stability-modulating properties.

The visually apparent shift from pale brown to dark reddish-brown aligns with the UV-visible absorption spectra findings, confirming the synthesis and maturation of the AgNPs. This visual observation adds a qualitative dimension to the comprehensive characterization of *Coriandrum sativum*-mediated AgNPs, further validating their successful formation and stabilization. UV-visible absorption spectroscopy analysis of the synthesized silver nanoparticles (AgNPs) revealed a distinct absorption peak at 450 nm, confirming the successful synthesis and stabilization of the nanoparticles [18,19]. The well-defined and narrow nature of this absorption peak indicates a uniform size distribution of the AgNPs, underscoring the reproducibility of the green synthesis process [20]. These findings are particularly significant because they highlight the efficacy of environmentally friendly methods for AgNP synthesis. This method holds promise for diverse applications across the biomedical, cellular imaging, cosmetics, drug delivery, food, and agrochemical industries [21]. Notably, the utilization of

biomolecules derived from various plant parts and microbial species as both reducing and capping agents in the synthesis process underscores the eco-friendly nature of AgNP production [22]. Ast-AgNPs are polyform, quasi-spherical, rectangular, and triangular, according to the TEM micrograph of the AgNPs made using *Asterarcys sp.* The average size of the nanoparticles, which ranged in size from 20 to 100 nm, was determined to be 52 nm [23]. According to other researchers, the nanoparticles had a somewhat broad range of sizes and were spherical or hexagonal [24].

Concentration-dependent antibacterial effects were observed for *C. sativum* AgNPs against *Staphylococcus aureus*, *Escherichia coli*, *Pseudomonas sp.*, and *Klebsiella sp.* The increased zones of inhibition at higher concentrations underscore the potential of *C. sativum* AgNPs as effective antibacterial agents against urinary tract infection pathogens [25]. Similarly, AgNPs synthesized from *Nepeta pogonosperma* extract exhibited antibacterial activity against a range of pathogens, including *Pseudomonas aeruginosa*, *Acinetobacter baumannii*, *Escherichia coli*, *Staphylococcus aureus*, *Klebsiella pneumoniae*, *Proteus mirabilis*, and *Enterococcus faecalis* [26]. Moreover, AgNPs produced by both gram-positive and gram-negative bacteria demonstrated significant antibacterial activity, particularly against *Klebsiella pneumoniae*, and inhibited biofilm formation, indicating their potential as antibacterial agents for respiratory tract infections [27]. Additionally, AgNPs derived from the ethanolic extract of *Allium sativum* exhibited antibacterial activity against *Escherichia coli* and *Staphylococcus aureus*, with larger inhibition zones than those of the plant extract alone [28]. Overall, these collective findings strongly support the potential use of AgNPs, especially those sourced from natural origins, as effective antibacterial agents against a variety of pathogens.

Antioxidants help to protect the human body against the damage caused by free radicals. There is a huge record that medicinal plants have efficient anti-oxidant, anti-inflammatory, antimicrobial, and anticancer properties in common. The polyphenols present in the *C. sativum* increased the activities of antioxidant enzymes, where the compounds are effectively responsible for the suppression of hydrogen peroxide and DPPH-induced oxidative stress [29]. *C. sativum* AgNPs exhibit significant antioxidant activity across various assays, highlighting their potential as natural antioxidants. In the DPPH scavenging assay, *C. sativum* AgNPs displayed substantial activity, with a maximum scavenging percentage of 88.6% at 50 µg/mL. This efficacy was comparable to or even superior to that of the standard antioxidant ascorbic acid, suggesting that *C. sativum* AgNPs could serve as effective natural antioxidants. Moreover, the H₂O₂ scavenging activity of *C. sativum* AgNPs was noteworthy at all concentrations, indicating their ability to neutralize hydrogen peroxide radicals. The scavenging activity increased consistently with increasing concentration, mirroring the behaviour of the standard antioxidant (ascorbic acid). In the FRAP assay, although the standard generally presented slightly higher values, *C. sativum* AgNPs demonstrated concentration-dependent ferric-reducing antioxidant potential, further confirming their antioxidant capabilities.

Previous studies have confirmed these findings, indicating that green-synthesized silver nanoparticles, including those derived from *C. sativum*, possess free radical scavenging activity [30]. The IC₅₀ values ranging from 15.63 mg/L to 48.96 ± 0.84 µg/mL suggest the ability of AgNPs to scavenge free radicals [31]. Additionally, the AgNPs showed significant antioxidant activity in various assays, such as the β-carotene linoleic acid lipid peroxidation assay, and exhibited dose-dependent antioxidant activity against DPPH radicals [32, 33].

The concentration-dependent increase in BSA denaturation percentages in the presence of *C. sativum* AgNPs indicates their potential effect on protein denaturation. The denaturation percentages were comparable to or greater than those observed with the standard diclofenac sodium. *C. sativum* AgNPs had concentration-dependent effects on egg albumin denaturation, with notable effects at relatively high concentrations. At 50 µg/mL, the denaturation effect of the *C. sativum* AgNPs was more pronounced than that of the standard. Furthermore, *C. sativum* AgNPs exhibited a concentration-dependent membrane stabilization effect, surpassing the standard at higher concentrations. At 50 µg/mL, the percentage of *C. sativum* AgNPs that stabilized the membrane was 86.9%, indicating their potential to stabilize biological membranes.

The anti-inflammatory activity of green-synthesized AgNPs has been reported in many previous studies. These nanoparticles inhibit the production of proinflammatory cytokines and reactive oxygen species (ROS) by suppressing the NF- κ B and cyclooxygenase-2 pathways [34]. Metal nanoparticles such as silver nanoparticles are designed to be small enough to pass through biological barriers and allow label-free monitoring of their interactions with cells [35].

Biogenic AgNPs synthesized from honeyberry and *Ageratum conyzoids* have shown protective effects against neuroinflammation and oxidative stress by targeting the toll-like receptor 4 (TLR4)/MyD88 and nuclear factor-E2-related factor 2 (Nrf2)/heme oxygenase-1 (HO-1) signalling pathways [36,37]. Additionally, AgNPs synthesized from rosa and jasminum extracts have demonstrated impressive anti-inflammatory activity in vitro [35]. These studies collectively underscore the potential of green-synthesized AgNPs as nanomedicines for the treatment of inflammatory diseases.

Limitations

The comprehensive analysis of the results underscores the multifaceted potential of *Coriander sativum*-mediated silver nanoparticles. The antibacterial and antioxidant activities of these compounds, along with their impact on protein denaturation and membrane stabilization, make them promising candidates for various biomedical and environmental applications. Future research could explore the mechanism underlying these observed effects and further optimize the synthesis process for enhanced performance in specific applications. Additionally, cell line and in vivo studies could provide valuable information on the safety and efficacy of these nanoparticles in real biological systems.

Conclusion

This study elucidates the green synthesis of silver nanoparticles (AgNPs) utilizing *Coriandrum sativum* extract, providing valuable insights into their synthesis kinetics, antibacterial efficacy, and antioxidant properties. Green synthesized AgNPs exhibited notable results in every parameter, where the research contributes to the understanding of their potential applications in diverse biomedical and therapeutic domains, emphasizing their significance in nanobiotechnology for future exploration and product development including antibacterial ointments and gels.

Acknowledgements

The authors are grateful to the Centre for Global Health Research, Saveetha Medical College and Hospitals, Saveetha Institute Medical and Technical Sciences, Chennai-602105, Tamil Nadu, India, for providing a research facility to carry out the entire research work.

Conflict of Interests

The authors declare that they have no conflicts of interest.

References

- [1]. Mancuso G, Midiri A, Gerace E, Marra M, Zummo S, Biondo C. 2023, Urinary tract infections: The current scenario and future prospects. *Pathogens*.12: 623. doi:10.3390/pathogens12040623
- [2]. England NHS. NHS England » New awareness campaign to help reduce hospital admissions for urinary tract infections. [cited 11 Mar 2024]. Available: <https://www.england.nhs.uk/2023/10/new-awareness-campaign-to-help-reduce-hospital-admissions-for-urinary-tract-infections>
- [3]. Yang X, Chen H, Zheng Y, Qu S, Wang H, Yi F. 2022, Disease burden and long-term trends of urinary tract infections: A worldwide report. *Front Public Health*. 10. doi:10.3389/fpubh.2022.888205
- [4]. Paul R. 2018, State of the globe: Rising antimicrobial resistance of pathogens in urinary tract infection. *J Glob Infect Dis*. 10: 117–118. doi:10.4103/jgid.jgid_104_17
- [5]. Sánchez SV, Navarro N, Catalán-Figueroa J, Morales JO. 2021, Nanoparticles as potential novel therapies for urinary tract infections. *Front Cell Infect Microbiol*.11. doi:10.3389/fcimb.2021.656496
- [6]. Qindeel M, Barani M, Rahdar A, Arshad R, Cucchiarini M. 2021, Nanomaterials for the diagnosis and treatment of urinary tract infections. *Nanomaterials (Basel)*. 211: 546. doi:10.3390/nano11020546
- [7]. Yin IX, Zhang J, Zhao IS, Mei ML, Li Q, Chu CH. 2020, The antibacterial mechanism of silver nanoparticles and its application in dentistry. *Int J Nanomedicine*.15: 2555–2562. doi:10.2147/ijn.s246764
- [8]. Divya M, Kiran GS, Hassan S, Selvin J. 2019, Biogenic synthesis and effect of silver nanoparticles (AgNPs) to combat catheter-related urinary tract infections. *Biocatal Agric Biotechnol*. 18: 101037. doi:10.1016/j.bcab.2019.101037
- [9]. Alsubki R, Tabassum H, Abudawood M, Rabaan AA, Alsobaie SF, Ansar S. 2021, Green synthesis, characterization, enhanced functionality and biological evaluation of silver nanoparticles based on *Coriander sativum*. *Saudi J Biol Sci*. 2021;28: 2102–2108. doi:10.1016/j.sjbs.2020.12.055
- [10]. Rajeshkumar S, Tharani M, Jeevitha M, Santhoshkumar J. 2019, Anticariogenic activity of fresh aloe Vera gel mediated copper oxide nanoparticles. *Indian J Public Health Res Dev*. 10: 3664. doi:10.5958/0976-5506.2019.04158.5
- [11]. Sobhani Z, Mohtashami L, Amiri MS, Ramezani M, Emami SA, Simal-Gandara J. 2022, Ethnobotanical and phytochemical aspects of the edible herb *Coriandrum sativum* L. *J Food Sci*. 87: 1386–1422. doi:10.1111/1750-3841.16085
- [12]. Prachayasittikul V, Prachayasittikul S, Ruchirawat S, Prachayasittikul V. 2018, Coriander (*Coriandrum sativum*): A promising functional food toward the well-being. *Food Res Int*. 105: 305–323. doi:10.1016/j.foodres.2017.11.019
- [13]. Salem MA, Manaa EG, Osama N, Aborehab NM, Ragab MF, Haggag YA, et al. 2022, Coriander (*Coriandrum sativum* L.) essential oil and oil-loaded nanoformulations as an anti-aging potentiality via TGFβ/SMAD pathway. *Sci Rep*. 12: 1–15. doi:10.1038/s41598-022-10494-4
- [14]. Al-Marzoqi AH, Hameed IH, Idan SA. 2015, Analysis of bioactive chemical components of two medicinal plants (*Coriandrum sativum* and *Melia azedarach*) leaves using gas chromatography-mass spectrometry (GC-MS). *African Journal of Biotechnology*. Oct 23;14(40):2812-30. doi: 10.5897/AJB2015.14956
- [15]. Sharma SK, Singh AP. 2012, In vitro antioxidant and free radical scavenging activity of *Nardostachys jatamansi* DC. *J Acupunct Meridian Stud*. 5: 112–118. doi:10.1016/j.jams.2012.03.002
- [16]. Rajeshkumar S, Malarkodi C, Vanaja M, Annadurai G. 2016, Anticancer and enhanced antimicrobial activity of biosynthesized silver nanoparticles against clinical pathogens. *Journal of molecular structure*. 15;1116:165-73.
- [17]. Bhatti MZ, Ali A, Ahmad A, Saeed A, Malik SA. 2015, Antioxidant and phytochemical analysis of *Ranunculus arvensis* L. extracts. *BMC Res Notes*. 8: 279. doi:10.1186/s13104-015-1228-3
- [18]. Devadharshini R, Karpagam G, Pavithra K, Kowsalya S, Priya PM, Ramachandran AM. 2023, Green synthesis of silver nanoparticles. *Microbiol*

Res J Int. 33: 1–9.
doi:10.9734/mrji/2023/v33i51380

[19]. Tharani M, Rajeshkumar S, Al-Ghanim KA, Nicoletti M, Sachivkina N, Govindarajan M. 2023, *Terminalia chebula*-Assisted Silver Nanoparticles: Biological Potential, Synthesis, Characterization, and Ecotoxicity. *Biomedicines*. 11. doi:10.3390/biomedicines11051472

[20]. Qaeed MA. 2023, Review of Biological methods of AgNPs Synthesis. *Journal of Chemistry and Nutritional Biochemistry*. 4. doi:10.48185/jcnb.v4i1.793

[21]. Guzmán K, Kumar B, Grijalva M, Debut A, Cumbal L. 2022, Ascorbic acid-assisted green synthesis of silver nanoparticles: pH and stability study. *Green Chemistry - New Perspectives*. IntechOpen; doi:10.5772/intechopen.107202

[22]. Chinnathambi A, Alharbi SA, Joshi D, Saranya, Jhanani GK, On-uma R, et al. 2023, Synthesis of AgNPs from leaf extract of *Naringi crenulata* and evaluation of its antibacterial activity against multidrug resistant bacteria. *Environ Res*. 216: 114455. doi:10.1016/j.envres.2022.114455

[23]. Choudhary S, Kumawat G, Khandelwal M, Khangarot RK, Saharan V, Nigam S, Harish. 2024, Phyco-synthesis of silver nanoparticles by environmentally safe approach and their applications. *Scientific Reports*. 14(1):9568. doi.org/10.1038/s41598-024-60195-3

[24]. Soleimani M, Habibi-Pirkoohi M. 2017, Biosynthesis of silver nanoparticles using *Chlorella vulgaris* and evaluation of the antibacterial efficacy against *Staphylococcus aureus*. *Avicenna journal of medical biotechnology*. 9(3):120. PMID: PMC5501138.

[25]. Antioxidant and antibacterial activities of *Allium sativum* ethanol extract and silver nanoparticles. 2023, *Tropical Journal of Natural Product Research*. 7. doi:10.26538/tjnpr/v7i6.5

[26]. Ebrahimzadeh MA, Barani A, Habibian AH, Goli HR, Alizadeh SR. 2023, Overcoming multidrug-resistant bacteria and fungi by green synthesis of AgNPs using *Nepeta pogonosperma* extract, optimization, characterization and evaluation of antibacterial and antifungal effects.

Eur J Chem. 14: 254–263.
doi:10.5155/eurjchem.14.2.254-263.2404

[27]. Asgarpanah J, Kazemivash N. 2012, Phytochemistry, pharmacology and medicinal properties of *Coriandrum sativum* L. *African Journal of Pharmacy and Pharmacology*. 22;6(31):2340-5. doi:10.5897/AJPP12.901

[28]. Ali Ahmed S, Mahmood Hasan H, Ghassan Sweedan E. 2023, Antibacterial action of AgNPs produced from different isolates of gram-positive and gram-negative bacteria on biofilm of *Klebsiella pneumoniae* isolated from RTI. *Biomed (Trivandrum)*. 43: 983–987. doi:10.51248/v43i3.2813

[29]. Mudhafar M, Alsailawi HA, Zorah M, Karhib MM, Zainol I, Kadhim FK. Biogenic Synthesis and Characterization of AgNPs Using CEPS: Cytotoxicity and Antibacterial Activities. 2023, *Adv Res Fluid Mech Therm Sci*. 106: 65–75. doi:10.37934/arfmts.106.1.6575

[30]. Fereydani M, Larijani K, Azizian F. 2023, Green synthesis of silver nanoparticles from *Polygonum aviculare* L. extract, evaluation of antibacterial, antioxidant activity. doi:10.22541/au.168735783.36916760/v1

[31]. Dua TK, Giri S, Nandi G, Sahu R, Shaw TK, Paul P. 2023, Green synthesis of silver nanoparticles using *Eupatorium adenophorum* leaf extract: characterizations, antioxidant, antibacterial and photocatalytic activities. *Chem Pap*. 77: 2947–2956. doi:10.1007/s11696-023-02676-9

[32]. Lakkim V, Reddy MC, Lekkala VVV, Lebaka VR, Korivi M, Lomada D. 2023, Antioxidant efficacy of green-synthesized silver nanoparticles promotes wound healing in mice. *Pharmaceutics*. 15: 1517. doi:10.3390/pharmaceutics15051517

[33]. Baran MF, Keskin C, Baran A, Hatipoğlu A, Yildiztekin M, Küçükaydin S, et al. 2023, Green synthesis of silver nanoparticles from *Allium cepa* L. peel extract, their antioxidant, antipathogenic, and anticholinesterase activity. *Molecules*. 28: 2310. doi:10.3390/molecules28052310

[34]. Kurup M, Kumar M, Ramanathan S, Chandra M. 2023, The biogenetic synthesis of metallic nanoparticles and the role they play in anti-inflammatory drug treatment. *Curr Drug Discov*

Technol. 20.
doi:10.2174/1570163820666230718123544
[35]. Singh S, Sharma K, Sharma H. 2024, Green extracts with metal-based nanoparticles for treating inflammatory diseases: A review. *Curr Drug Deliv.* 21: 544–570.
doi:10.2174/1567201820666230602164325
[36]. Sharma A, Sanjay, Jaiswal V, Park M, Lee H-J. 2023, Biogenic silver NPs alleviate LPS-induced neuroinflammation in a human fetal brain-derived

cell line: Molecular switch to the M2 phenotype, modulation of TLR4/MyD88 and Nrf2/HO-1 signalling pathways, and molecular docking analysis. *Biomater Adv.* 148: 213363.
doi:10.1016/j.bioadv.2023.213363
[37]. Xu Z, Zha X, Ji R, Zhao H, Zhou S. 2023, Green biosynthesis of silver nanoparticles using aqueous extracts of *Ageratum conyzoides* and their anti-inflammatory effects. *ACS Appl Mater Interfaces.* doi:10.1021/acsami.2c22114